Femtosecond photoisomerization of azobenzene-derivative binding to DNA

Tao Chen[a,c]*, Kazumasa Igarashi[a], Naoya Nakagawa[a], Keisaku Yamane[a], Taiga Fujii[b], Hiroyuki Asanuma[b] and Mikio Yamashita[a,*]

[a]Department of Applied Physics, Graduate School of Engineering, Hokkaido University and Core Research for Evolutional Science and Technology (CREST), Japan Science and Technology Agency (JST), Kita-13, Nishi-8, Kita-ku, Sapporo 060-8628, Japan

[b]Department of Molecular Design and Engineering, Graduate School of Engineering, Nagoya University and Core Research for Evolutional Science and Technology (CREST), Japan Science and Technology Agency (JST), Nagoya 464-8603, Japan

[c]School of Electronics & Information Engineering, Xi'an Jiaotong University, Xi'an, 710049 China

*Corresponding author to provide: Tel: +81-11-7066705, Fax: +81-11-7067887

Email: taochen@stu.xjtu.edu.cn; mikio@eng.hokudai.ac.jp

Abstract: Ultrafast photoisomerization and relaxation dynamics of *trans* (T) 4'-methylthioazobenzene (AzD) binding to double-strand DNA (T-AzD-dsDNA) as well as single-strand DNA (T-AzD-ssDNA) and T-AzD were investigated by the measurement of femtosecond absorbance changes on S_2^T excitation (400 nm) with the rate equation analysis. All the solutions showed the fast (τ_1, A_1) and slow (τ_2, A_2) decay components and the offset component (A_3). The greatly different negative or positive absorbance change behaviors by the probe wavelength of 400 or 420 nm for the T-AzD solution were attributed to the remarkable dependence of the absorption cross-section difference between the T-isomer excited and ground states on the probe wavelength and of that between the *cis* (C)- and T-isomer ground states. The significantly shorter S_2^T -state lifetimes τ_1 for T-AzD-dsDNA and T-AzD-ssDNA were observed to be 30 and 60 fs,

respectively, compared with that (220 fs) of T-AzD. This is presumably attributed to the intramolecular electron transfer from DNA bases to T-AzD in T-AzD-DNAs, suggesting the first observation of electron transfer in an ultrafast photoisomerization system interacting with DNA. While, the kinetic rate $k_{2,1}^{T,I}$ from the S_2^T state to the bottleneck intermediate state $I_1^{T,C}$ of the initial process in the T to C photoisomerization and the $I_1^{T,C}$-state lifetime τ_2 hardly changed like 1.3×10^{11}, 1.4×10^{11} and 1.6×10^{11} s^{-1} and like 6.7, 6.2 and 6.0 ps, respectively. The latter implies that the birth time of the C-isomer is almost the same for all the solutions. Furthermore, the T-to-C photoisomerization rate $\eta^{T,C}$ by single-shot excitation was determined from A_3 to be 1.2, 0.36 and 0.22 % at the hundred-nJ pulse energy level, indicating that the T-AzD molecule is one of the most efficient T-to-C photoisomerization molecules. The decrease of $\eta^{T,C}$ in T-AzD-DNAs is due to the dramatic shortening of the excited-state lifetime τ_1.

Keywords: Photoisomerization, Femtosecond phenomena, Ultrafast biomolecular spectroscopy, Intramolecular electron transfer.

1. Introduction

Recently, much attention has bee focused on artificial control of bio-chemical reactions [1]. Therefore, a number of photoisomerization groups have been taken as one of reactions to be controlled [2]. Among them, reversible control of DNA hybridization using photoisomerization of binding azobenzene (Az) derivatives by light irradiation of different wavelengths has attracted considerable attention because of ease of the preparation and efficient photoisomerization probability [1,3-5]. In addition, Asanuma *et al*. have applied the reversible control technique for photoregulation of gene expression *in vitro* to demonstrate a possibility as the widely available method in a living system [6]. Furthermore, a new azobenzene derivative, 4'-methylthioazobenzene (we call AzD), without giving the optical damage to the living cell, has been demonstrated, where *trans* (T) to *cis* (C) photoisomerization occurs by CW-lamp irradiation at the longer wavelength than 400 nm (S_2 excitation) and C-to-T photoisomerization occurs at around 520 nm (S_1 excitation) [7,8]. However, we have no knowledge of ultrafast electronic excited-state dynamics of the AzD binding to DNA (AzD-DNA) as well as the AzD, though for Az related compounds extensive studies on photoisomerization mechanisms such as rotation, inversion and concerted inversion processes have been carried out to clarify the relation between these processes and the excitation bands [9-11].

The purpose of this paper is to reveal the competitive femtosecond-to-picosecond processes of T-to-C photoisomerization and relaxation from the second electronic excited-state S_2^T of *trans* AzD-(double-strand)DNA (T-AzD-dsDNA) solution, *trans* AzD-(single-strand)DNA (T-AzD-ssDNA) solution and *trans* AzD (T-AzD) solution. Then, we investigated the transient absorption behaviors of those solutions with the rate equation analysis [12,13]. We also obtain the T-to-C photoisomerization rate $\eta^{T,C}$ per

femtosecond pump pulse, the yielding rate of the photoproduct C-isomer by single-shot excitation, and discuss the physical origin of the difference of the $\eta^{T,C}$ for three solutions. The rate $\eta^{T,C}$ will become one of the most important parameters for coherent control [14] of photoisomerization in AzD-DNA solutions by single-shot excitation of a shaped femtosecond pulse [15]. This is because its instant, efficient control technique may enable us to manipulate quasi-simultaneously and site-selectively bio-molecular functions at many local-desired points of a high order molecular-structure system and hence to offer a new tool for the bio-medical technology and the DNA nanotechnology [16].

2. Experimental setup

The employed AzD and AzD-DNAs (Nihon Techno Service Co.) were synthesized and purified by the procedure described in ref. [7]. The AzD solution in dimethylsulfoxide (DMSO, spectroscopic grade) was at the concentration of 4.0 mM or 8.0 mM. The AzD-ssDNA and AzD-dsDNA solutions were the single-strand form of 5'-ACGA<u>S</u>CTCA-3' (<u>S</u> denotes AzD) and its double-strand form (see Fig. 1(a)) dissolved in buffer solution at the concentration of 4 mM. All the samples were prepared as the pure T-form by being kept at 90 ℃ for 10 minutes prior to the experiment (less than 1.2 % C-form remained for AzD). The purity and absorption cross section of the samples were confirmed by measurements of high-performance liquid chromatography (HPLC), the absorption spectrum and nuclear magnetic resonance. Those absorption spectra for both the T- and C-forms are shown in Fig. 1(b).

The experimental setup similar to that in refs. [12,13] was used to measure transient absorbance changes $\Delta OD(t)$ by the noncollinear femtosecond pump-probe technique. The ultrafast laser source is a 30-fs, 2.5-mJ Ti:sapphire laser-amplifier system which provides 815 nm pulses at a repetition rate of 1 kHz. Two 100-μm BBO crystals and two chirped

mirror pairs were used to generate independently the second harmonics at 408 nm for 50-fs pump pulses with different energies (80-200 nJ), and at 400 or 420 nm for probe pulses (~5 nJ), respectively. A rapid-scan detection method was used to record the transient signal $\Delta OD(t)$, which can avoid the influence of the long-term laser energy fluctuation [17]. A 0.2-mm (=*d*) thick, 132-μL rotating cell was used to save the quantity of the valuable DNA samples and avoid the accumulation effect of the photoisomerization product by repetitive pump pulses. The rotational velocity was high enough to make sure the pure T-form as the initial state of the sample solution for each pump pulse.

3. Results and discussion

3.1 AzD solution

Figure 2(a) shows the transient absorbance changes $\Delta OD^{A}_{400}(t)$ measured at 400 nm probe and 408 nm pump wavelengths with different pump energies from 40 to 200 nJ for T-AzD in DMSO (4 mM concentration). Figure 2(a') shows the corresponding time-axis expanded ones. We find that after the negative peak rapidly decreased within a few hundred femtoseconds, the negative change $\Delta OD^{A}_{400}(t)$ mostly decreases until sub-10 picoseconds. Finally it shows a negative offset at about 40 ps. Those negative changes increase with increasing the pump energy including the offset, while those profiles do not change. We also confirmed the similar result at the 8 mM concentration. Figure 2(b) shows the absorbance change $\Delta OD^{A}_{420}(t)$ measured at 420 nm probe wavelength at the 200 nJ pump energy as well as the 400 nm one $\Delta OD^{A}_{400}(t)$ (Fig. 2(b') is the corresponding time-axis expanded one). The $\Delta OD^{A}_{420}(t)$ is very different from the $\Delta OD^{A}_{400}(t)$. After showing the small negative peak within few hundred femtoseconds, the $\Delta OD^{A}_{420}(t)$ rapidly changes to the somewhat small positive peak within few hundred femtoseconds and then decays

from the positive to the negative region within sub-10 picoseconds. Finally, it shows the small negative offset at about 30 ps. This difference is similar to the result observed at S_2^T -band probe wavelengths under S_2^T band excitation for *trans* 4-(dimethylamino)azobenzene dissolved in ethanol [18], except for the negative peak observed at around zero-time delay for the $\Delta OD_{420}^{A}(t)$, which is due to the fact that the present instrument response is much shorter (50 fs) than that (600 fs) in ref. [18].

These results can be well understood by applying the analytical results of the rate equations (see refs. [12, 13]) describing the population dynamics of the ground states S_0^T and S_0^C as well as the second excited states S_2^T and the "bottleneck" intermediate state $I_1^{T,C}$ [19,20] (Fig. 3), which involve in the ultrafast processes of photoisomerization of T-AzD and T-AzD-DNAs. The analytical result showed that the absorbance change $\Delta OD_i^m(t)$ has three components such as $A_1 \exp(-t/\tau_1) + A_2 \exp(-t/\tau_2) + A_3$. The fast component is due to the sum of the transition from the second excited state S_2^T to the ground state S_0^T by the internal conversion process (the kinetic rate $k_{2,0}^T$) and the transition from S_2^T state to the "bottleneck" intermediate state $I_1^{T,C}$ [19] (the kinetic rate $k_{2,1}^{T,I}$) mainly leading to the photoproduct C-isomer. That is, we assumed that molecules returning to the ground state S_0^T of the reactant T-isomer are mostly via the internal conversion process but hardly via the intermediate state $I_1^{T,C}$ presumably because of a relatively large potential energy barrier for the $I_1^{T,C}$-to S_0^T transition [12,13]. The S_2^T state lifetime τ_1 equals the inverse of the sum of $k_{2,0}^T$ and $k_{2,1}^{T,I}$. The amplitude A_1 depends on the differences between the absorption cross section $\sigma_{2,n}^T$ (or $\sigma_{1,n}^I$) of the excited state S_2^T (or $I_1^{T,C}$) and that $\sigma_{0,2}^T$ of the ground state S_0^T at the probe wavelength as well as the difference $\Delta\sigma_{0,2}^{C,T} = \sigma_{0,2}^C - \sigma_{0,2}^T$

between the absorption cross section $\sigma_{0,2}^{T}$ of the ground state S_0^T of the reactant T-isomer and that $\sigma_{0,2}^{C}$ of the ground state S_0^C of the photoproduct C-isomer at the probe wavelength. We assumed that the slow component is mainly due to the transition from the intermediate state $I_1^{T,C}$ to the ground state S_0^C of the photoproduct [12,13]. The $I_1^{T,C}$-state lifetime τ_2 equals the inverse of the kinetic rate $k_{1,0}^{I,C}$. The amplitude A_2 depends on the difference $\Delta\sigma_{1,n:0,2}^{I,C} = \sigma_{1,n}^{I} - \sigma_{0,2}^{C}$ between the absorption cross section $\sigma_{1,n}^{I}$ of the intermediate state $I_1^{T,C}$ and that $\sigma_{0,2}^{C}$ of the photoproduct ground state S_0^C. The offset is due to the photoproduct isomer C and the amplitude A_3 is proportional to the ground-state absorption cross-section difference $\Delta\sigma_{0,2}^{C,T}$ according to the equation $A_3 = C \times S_{0,2}^{T} \times n_0^T(0) \times k_{2,1}^{T,I} \times \tau_1 \times \Delta\sigma_{0,2}^{C,T}$ (also $A_3 = C \times n_0^C(\infty) \times \Delta\sigma_{0,2}^{C,T}$ [12,13]), where $C = d/\ln 10$, $n_0^T(0)$ is the population in the ground state S_0^T corresponding to the initial concentration of the reactant T-isomer, $n_0^C(\infty)$ is the population in the ground state S_0^C corresponding to the concentration of the photoproduct C-isomer, and $S_{0,2}^{T}$ is the effective excitation probability considering the pumping saturation ($S_{0,2}^{T} = 1 - \exp(-P_{0,2}^{T})$ and $P_{0,2}^{T} = \sigma_{0,2}^{T}(\lambda_{pump}) \times E_{pump}/(\hbar\omega_{pump}) \times S_{pump}$, where E_{pump}, $\hbar\omega_{pump}$ and S_{pump} are the pump pulse energy, photon energy and beam cross section, respectively). Therefore, the difference between $\Delta OD_{400}^{A}(t)$ and $\Delta OD_{420}^{A}(t)$ is due to the following differences of the related absorption cross sections: in $\Delta OD_{420}^{A}(t)$ the $A_{2,420}$ is positive due to the $\Delta\sigma_{1,n:0,2}^{I,C} > 0$ at 420 nm and the offset $A_{3,420}$ is small negative due to the $\Delta\sigma_{0,2}^{C,T} < 0$ but the small difference at 420 nm, while in $\Delta OD_{400}^{A}(t)$ the $A_{2,400}$ is negative due to the $\Delta\sigma_{1,n:0,2}^{I,C} < 0$ at 400 nm and the offset $A_{3,400}$ is large negative due to the $\Delta\sigma_{0,2}^{C,T} < 0$ but the large difference at 400 nm. The fact that $0 > \Delta\sigma_{0,2}^{C,T}$ (420 nm)$> \Delta\sigma_{0,2}^{C,T}$ (400 nm) corresponds to the

difference between the steady-state absorption spectrum of the ground state C-isomer and that of the ground state T-isomer at 420 and 400 nm (see Fig. 1(b)). That is, this difference of the offset_is confirmed from the measurement results that the ratio $A_{3,420}$/ $A_{3,400}$=0.33 from Fig. 2(b) is considerately close to the ratio $\Delta\sigma_{0,2}^{C,T}(420)$/ $\Delta\sigma_{0,2}^{C,T}(400)$=0.50 from Fig. 1(b) (the deviation may be due to the measurement errors of A_3 and $\Delta\sigma_{0,2}^{C,T}$).

Using the above mentioned three-component function and the instrument response measured from the two-photon absorption of the solvent, the measured $\Delta OD_{400}^{A}(t)$ was fitted to obtain the lifetimes τ_i (i =1 or 2), the relative amplitudes a_i ($a_i = |A_i| / \sum_{i=1}^{i=3} |A_i|$) ($i$ =1, 2 or 3), and the kinetic rate $k_{i,j}^{m,n}$ (i, j=0, 1 or 2, and m, n=T, C or I), which are summarized in Table I. The S_2^T -state lifetime of τ_1=220 fs is longer than that of 110 fs the T-Az in hexane [21] in which the T-Az molecule is the planar structure with the smaller size. The $I_1^{T,C}$ -state lifetime of τ_2=6.7 ps suggests that the C-isomer is yielded within about 7 ps after excitation by a 408-nm femtosecond pulse. The kinetic rate $k_{2,1}^{T,I}$ from the S_2^T state to the $I_1^{T,I}$ state and the corresponding transfer rate $T_{2,1}^{T,I} = k_{2,1}^{T,I} \times \tau_1$, which are obtained from the above-mentioned relation between the measured A_3 and the $k_{2,1}^{T,I}$, are 1.3×10^{11} s^{-1} and 2.9 %, respectively. Furthermore, the most interesting parameter, the photoisomerization rate per pump pulse $\eta^{T,C} = n_0^C(\infty)/n_0^T(0) = S_{0,2}^T \times k_{2,1}^{T,I} \times \tau_1$ [12,13], indicating the rate of the photoproduct C-isomer to be yielded by single-shot excitation of a femtosecond optical pulse, is obtained to be 1.2 % at the 408-nm pump pulse energy of 120 nJ. This result suggests that the AzD is the much more efficient T-to-C photoisomerization molecule as a photoregulator compared to the already-reported Az

and its derivatives [3-6], with the advantage of the pump wavelength without damaging the living cell [7,8].

3.2 AzD-DNA solutions and comparison

Figures 4(a) and (b) show the transient absorbance changes $\Delta OD_{400}^{(s)}(t)$ and $\Delta OD_{400}^{(d)}(t)$ measured at the 400-nm probe and 408-nm pump wavelengths with different pump pulse energies for T-AzD-ssDNA buffer solution and T-AzD-dsDNA buffer solution at a concentration of 4 mM, respectively. Figures 4(a') and (b') show the corresponding time-axis expanded ones, respectively. Figure 4 (c) shows the absorbance changes $\Delta OD_{400}^{A}(t)$ at 120-nJ pump, $\Delta OD_{400}^{(s)}(t)$ and $\Delta OD_{400}^{(d)}(t)$ at 130-nJ pump as well as the corresponding time-axis expanded ones (c'). In the same way as the case of T-AzD solution, in both the T-AzD-DNA solutions also the $\Delta OD_{400}^{(s)}(t)$ and $\Delta OD_{400}^{(d)}(t)$ show the three negative components, the sub-100 fs (τ_1, A_1), the sub-10 ps (τ_2, A_2) and the offset A_3 in the same time region of fs-to-ps but those absolute amplitudes are about half. In addition, the fast component becomes more dominant and the time constant τ_1 becomes shorter, while the offset amplitude $|A_3|$ decreases. This tendency becomes more remarkable for AzD-dsDNA. And those absorbance changes increase negatively with increasing the pump pulse energy, while keeping those temporal profiles the almost same. Similarly, the $\Delta OD_{400}^{(s)}(t)$ and $\Delta OD_{400}^{(d)}(t)$ were fitted numerically. The obtained lifetimes τ_i, the relative amplitudes a_i and the kinetic rate $k_{i,j}^{m}$ are summarized in Table I, including the S_2^T-to-$I_1^{T,C}$ kinetic rate $k_{2,1}^{T,I}$, the corresponding transfer rate $T_{2,1}^{T,I}$ and the T-to-C photoisomerization rate per pump pulse $\eta^{T,C}$.

Comparison among the three cases makes clear the following points: (i) in order of T-AzD, T-AzD-ssDNA and T-AzD-dsDNA, the S_2^T-state lifetime τ_1 significantly decreases

from 220, 60 to 30 fs while the S_2^T-to-$I_1^{T,C}$ kinetic rate $k_{2,1}^{T,I}$ and the $I_1^{T,C}$-state lifetime τ_2 hardly change like 1.3×10^{11}, 1.4×10^{11} and 1.6×10^{11} s^{-1}, and like 6.7, 6.2 and 6.0 ps, respectively. The dramatic shortening of the S_2^T-state lifetime in T-AzD-DNAs may be associated with the intramolecular electron transfer [22,23] from DNA bases to T-AzD, which is the fist observation in an ultrafast photoisomerization system interacting with DNA. The lifetime shortening due to the difference of the solvent between T-AzD and T-AzD-DNAs is excluded. This is because several previous papers reported that the solvent only slightly changes the lifetime for T-Az related compounds [9, 18-21]. In addition, if the lifetime would be mainly changed by the difference of the solvent, the lifetimes would not change significantly by the difference between T-AzD-ssDNA and T-AzD-dsDNA because of the same solvents (buffer solutions). However, the experimental result shows significantly different lifetimes (60 and 30 fs) between T-AzD-ssDNA and T-AzD-dsDNA in spite of the same solvents. But, the further study, including the influence of such extremely fast intramolecular electron transfer on the potential barrier to the intermediate state, is needed. The result of the lifetime τ_2 indicates that the birth time of the photoproduct C-isomer is almost same (~7 ps) for the three cases. These findings suggest that in the experiment for photoisomerization coherent control of T-AzD-DNA solutions, 10-20 ps delay time of a 400-nm probe pulse after excitation by a 408-nm shaped pulse [15] is suitable. (ii) The T-to-C photoisomerization rate $\eta^{T,C}$ per pump pulse and hence the photoisomerization efficiency significantly decrease in AzD-DNA cases: e.g. $\eta^{T,C}$=0.36 and 0.22 % at the 130-nJ pump pulse energy for T-AzD-ssDNA and T-AzD-dsDNA, respectively. This is because the excited-state lifetime τ_1 greatly decreases, though the S_2^T-to-$I_1^{T,C}$ kinetic rate hardly changes. We confirmed that the tendency of the

$\eta^{T,C}$ decrease in order of T-AzD, T-AzD-ssDNA and T-AzD-dsDNA agrees with the evaluation result of the T-to-C photoisomerization quantum yield by the conventional CW-lamp irradiation method [24]. It seems that the physical origin of the difference in photoisomerization efficiency between T-AzD binding to DNAs and free T-AzD is completely different from that of the case in rotation-restricted and rotation-free Az derivatives [25]. In the latter case it was suggested that the relaxed states and probably trajectories for both the molecules are different on the potential energy surfaces of the excited states.

4. Conclusion

We clarified quantitatively femtosecond photoisomerization and relaxation processes from the second excited state S_2^T of T-AzD-dsDNA (the lifetime τ_1=30 fs) and T-AzD-ssDNA (the τ_1=60 fs) in buffer solutions as well as T-AzD in DMSO (the τ_1=220 fs) for the first time. We found that the observed remarkable dependence of the transient absorbance change on the probe wavelength on S_2^T excitation for the T-AzD solution is due to the fact that the absorption cross-section difference $\Delta\sigma_{1,n:0,2}^{I,C}$ between the intermediate and ground states as well as that $\Delta\sigma_{0.2}^{C,T}$ between the C-isomer and T-isomer ground states are highly sensitive to the probe wavelength. Furthermore, the offset component observed for all the solutions, which was found to be due to the photoproduct C-isomer, enables us to obtain the T-to-C photoisomerization rate per pump pulse. That is, 1.2 % of T-AzD molecules in the ground state S_0^T are isomerized to the C-form within about 7 ps by single-shot excitation of a 408-nm femtosecond pulse with energy of the hundred-nJ level, which implies one of the most efficient compounds as a photoregulator of DNA hybridization. While, for T-AzD-ssDNA solution and T-AzD-dsDNA solution 0.36 and 0.22 % are isomerized to the C-form within the almost same time by the same

single-shot excitation, respectively. This great decrease was found to be mainly due to the dramatic shortening of the exited S_2^T-state lifetime τ_1, which may be associated with the intramolecular electron transfer from DNA bases to T-AzD in AzD-DNAs.

Acknowledgments

This research was supported by Core Research for Evolutional Science and Technology (CREST), Japan Science and Technology. T. Chen would like to thank the support of government scholarship from China Scholarship Council and Prof. Jinhai Si of Xi'an Jiaotong University for offering the opportunity of studying in Yamashita CREST Lab. We would also like to thank Prof. Jun Takeda of Yokohama National University for introducing the rotating cell, and Prof. Kazuhiko Misawa of Tokyo University of Agriculture and Technology for help in rapid-scan system.

References

[1] S. Patnaik, P. Kumar, B.S. Garg, R. P. Gandhi, K. C. Gupta, Bio. Med. Chem. 15 (2007) 7840-7849.

[2] C. Dugae, L. Demange, Chem. Rev. 103 (2003) 2475-2532.

[3] H. Asanuma, X. G. Liang, H. Nishioka, D. Matsunaga, M. Liu, M. Komiyama, Nature Protocols 2 (2007) 203-212.

[4] H. Nishioka, X. G. Liang, H. Kashida, H. Asanuma, Chem. Comm. (Cambridge) (2007) 4354-4356.

[5] H. Nishioka, X. G. Liang, H. Asanuma, Chem. Eur. J. 16 (2010) 2054-2062.

[6] X. G. Liang, K. Fujioka, Y. Tsuda, R. Wakuda, and H. Asanuma, Nucleic Acids Symposium Series, 52 (2008) 19-20.

[7] T. Fujii, H. Kashida, H. Asanuma, Chem. Eur. J. 15 (2009) 10092-10102.

[8] K. Fujioka, T. Fujii, H. Kashida, X. G. Liang, H. Asanuma, presented at the twenty forth biofunctional chemistry symposium, Kyushu, Japan, 18-20 Sept. 2009.

[9] T. Fujino, S. Y. Arzhantsev, T. Tahara, Bull. Chem. Soc. Jpn 75 (2002) 1031-1040.

[10] C. -W. Chang, Y. -C. Lu, T. -T. Wang, E. W. -G. Diau, J. Am. Chem. Soc. 126 (2004) 10109-10118.

[11] L. Wang, W. Xu, C. Yi, X. Wang, J. Mol. Graph. Mod. 27 (2009) 792-796.

[12] A. Yamaguchi, N. Nakagawa, K. Igarashi, T. Sekikawa, H. Nishioka, H. Asanuma, M. Yamashita, Appl. Surf. Sci. 255 (2009) 9864-9868.

[13] T. Chen, A. Yamaguchi, K. Igarashi, N. Nakagawa, H. Nishioka, H. Asanuma, M. Yamashita, Jpn. J. Appl. Phys. (in submission),

[14] A. C. Florean, D. Cardoza, J. L. White, J. K. Lanyi, R. J. Sension, P. H. Bucksbaum, PNAS 106 (2009) 10896-10900.

[15] T. Tanigawa, Y. Sakakibara, S. Fang, T. Sekikawa, M. Yamashita, Opt. Lett. 34 (2009) 1696-1698.

[16] Y. Ito, E. Fukusaki, J. Mol. Catal. B 28 (2004) 155-166.

[17] K. Horikoshi, K. Misawa, R. Lang, K. Ishida, Opt. Commun. 259 (2006) 723-726.

[18] S. G. Mayer, C. L. Thomsen, M. P. Philpott, P. J. Reid, Chem. Phys. Lett. 314 (1999) 246-254.

[19] I. K. Lednev, T. -Q. Ye, R. E. Hester, J. N. Moore, J. Phys. Chem. 100 (1996) 13338-13341.

[20] I. K. Lednev, T. -Q. Ye, P. Matousek, M. Towrie, P. Foggi, F. V. R. Neuwahl, S. Umapathy, R. E. Hester, J. N. Moore, Chem. Phys. Lett. 290 (1998) 68-74.

[21] T. Fujino, S. Y. Arzhantsev, T. Tahara, J. Phys. Chem. A 105 (2001) 8123-8129.

[22] D. Banerjee, S. K. Pal, J. Phys. Chem. 112 (2008) 1016-1021.

[23] D. Reha, M. Kabelac, F. Ryjacek, J. Sponer, J. E. Sponer, M. Elstner, S. Suhai, P. Hobza, J. Am. Chem. Soc. 124, (2002) 3366-3376.

[24] G. Zimmerman, L. Y. Chow, U. J. Paik, J. Am. Chem. Soc. 80, (1958) 3528-3531.

[25] Y. -C. Lu, E. W. -G. Diau, J. Phys. Chem. A 109, (2005) 2090-2099.

Figure Caption

Fig. 1.(Color online) (a) Molecular structures and sequence of AzD-ssDNA and AzD-dsDNA [7,8]. (b) Absorption spectra of solutions of T- and C-AzD dissolved in DMSO and T- and C-AzD-DNAs dissolved in buffer.

Fig. 2.(Color online) (a) Measured dependence of transient absorbance changes on pump energy for T-AzD at 400 nm probe and 408 nm pump (inversed triangle), and (a') the corresponding time-axis expanded ones (inversed triangle). (b) The transient absorbance changes for T-AzD at 400 (black inversed triangle) and 420 (red circle) nm probes and 408 nm pump, and (b') the corresponding time-axis expanded ones, where the pump pulse energy were 200 nJ. The solid lines are the fitted theoretical results.

Fig.3.(Color online) Schematic electronic energy diagram of excited, bottleneck and ground states with relaxation and photoisomerization processes for T-AzD and T-AzD-DNAs.

Fig. 4. (Color online) Measured dependence of transient absorbance changes on pump energy ((a) and (b)) and their time-axis expanded ones ((a') and (b')) at 400 nm probe and 408 nm pump: (a) and (a') for T-AzD-ssDNA (circle); (b) and (b') for T-AzD-dsDNA (diamond). (c) Comparison of measured transient absorbance changes among T-AzD (blue inverse triangle)) at 120 nJ pump as well as T-AzD-ssDNA (black circle) and T-AzD-dsDNA (red diamond) at 130 nJ pump, and (c') their time-axis expanded ones, where the solid lines are the fitted theoretical results.

Figure 1

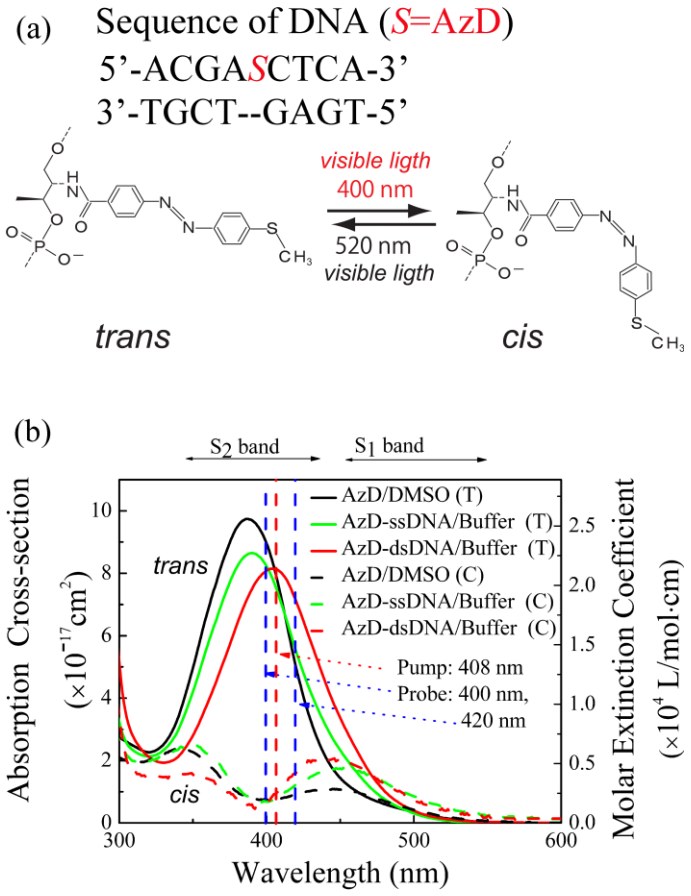
(a)
Sequence of DNA (S=AzD)
5'-ACGASCTCA-3'
3'-TGCT--GAGT-5'
visible ligth
400 nm
520 nm
visible ligth
trans
cis
(b)
S2 band
S1 band
AzD/DMSO (T)
AzD-ssDNA/Buffer (T)
AzD-dsDNA/Buffer (T)
AzD/DMSO (C)
AzD-ssDNA/Buffer (C)
AzD-dsDNA/Buffer (C)
Pump: 408 nm
Probe: 400 nm,
420 nm
trans
cis
Absorption Cross-section (×10^-17 cm^2)
Molar Extinction Coefficient (×10^4 L/mol·cm)
Wavelength (nm)

Figure 2

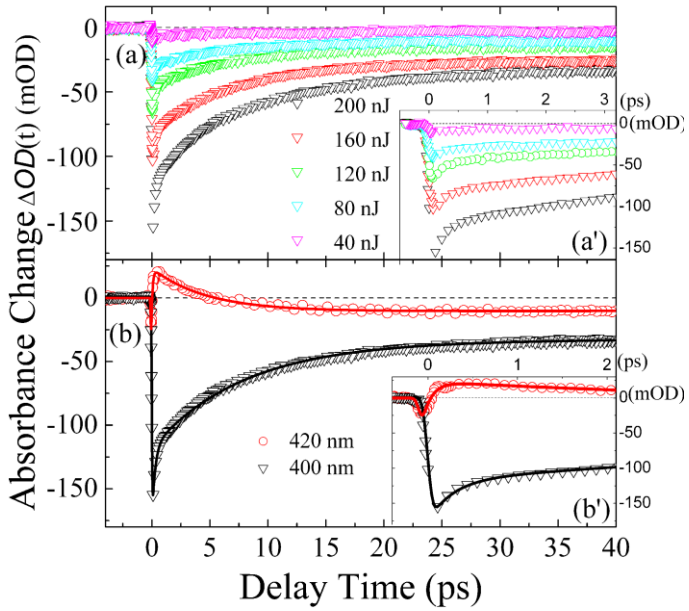

Figure 3

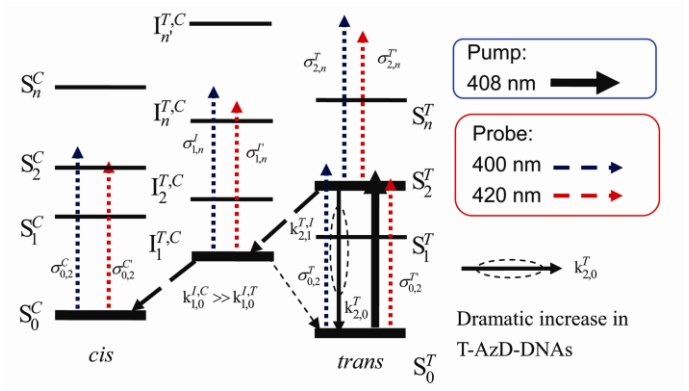

Figure 4

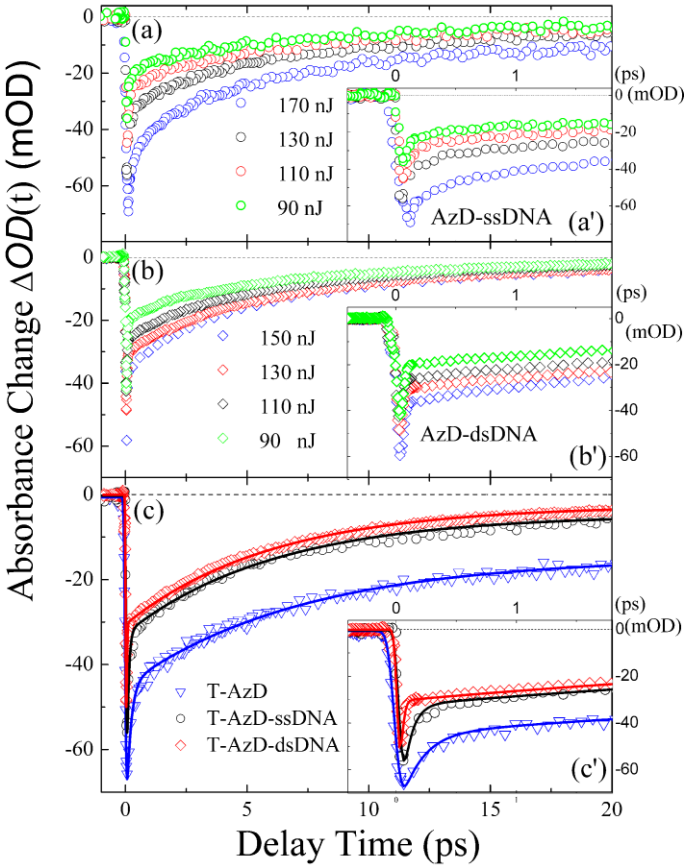
Absorbance Change ΔOD(t) (mOD)
Delay Time (ps)
(a)
170 nJ
130 nJ
110 nJ
90 nJ
AzD-ssDNA
(a')
(b)
150 nJ
130 nJ
110 nJ
90 nJ
AzD-dsDNA
(b')
(c)
T-AzD
T-AzD-ssDNA
T-AzD-dsDNA
(c')
(ps)
(mOD)

Table I. Lifetime τ_i, relative amplitudes $\mathbf{a}_i$, offset amplitude A_3, kinetic rate $k_{i,j}^{m,n}$, transfer rate $T_{2,1}^{T,I}$ and photoisomerization rate per pump pulse $\eta^{T,C}$ of T-AzD, T-AzD-ssDNA[a] and T-AzD-dsDNA[a]

	τ_1 (fs)	τ_2 (ps)	a_1 (%)	a_2 (%)	a_3 (%)	A_3 (mOD)	$k_{2,0}^{T}$ ($\times 10^{12}$ s^{-1})	$k_{2,1}^{T,I}$ ($\times 10^{11}$ s^{-1})	$k_{1,0}^{I,C}$ ($\times 10^{11}$ s^{-1})	$T_{2,1}^{T,I}$ (%)	$\eta^{T,C}$ (%)
T-AzD	220	6.7	41	40	19	-15	4.4	1.3	1.5	2.9	1.2(1.3[b])
T-AzD-ssDNA	60	6.2	59	35	6	-5.7	17	1.4	1.6	0.80	0.36
T-AzD-dsDNA	30	6.0	68	29	3	-3.6	38	1.6	1.7	0.43	0.22

[a]At the pump energy of 130 nJ except 120 nJ for T-AzD.

[b]Corresponding to the pump energy of 130 nJ